2021 43rd Annual International Conference of the
IEEE Engineering in Medicine & Biology Society (EMBC)
Oct 31 - Nov 4, 2021. Virtual Conference

Towards a Self-Powered ECG and PPG Sensing Wearable Device

Linran Zhao, Yaoyao Jia

Department of Electrical and Computer Engineering, The University of Texas at Austin, TX, U.S.A

***Abstract*—This paper presents a multifunctional sensor interface system-on-chip (SoC) for developing self-powered Electrocardiography (ECG) and Photoplethysmography (PPG) sensing wearable devices. The proposed SoC design consists of switch-capacitor-based LED driver and analog front-end (AFE) for PPG sensing, ECG sensing AFE, and power management unit for energy harvesting from Thermoelectric Generator (TEG), all integrated on a 2×2.5 mm^2 chip fabricated in 0.18-µm standard CMOS process. We have performed post-layout simulation to verify the functionality and performance of the SoC. The LED driver employs the switch-capacitor-based architecture, which charges a storage capacitor up to 2.1 V and discharges accumulated charge to pass instantaneous current up to 40 mA through a selected LED. The PPG AFE converts the resulting photodiode (PD) current to voltage output with adjustable gain of 114–120 dBΩ and input-referred noise of 119 pA_{RMS} within 0.4 Hz–10 kHz. The ECG AFE provides adjustable mid-band gain of 47-63 dB, low-cut frequency of 1.5–6.3 Hz, and input-referred noise of 7.83 μV_{RMS} within 1.5 Hz–1.2 kHz to amplify/filter the recorded ECG signals. The power management unit is able to perform sufficient energy harvesting with the TEG output voltage as low as 350 mV.**

I. Introduction

Cardiovascular-related diseases, such as Atrial Fibrillation (AFib) and Sudden Cardiac Arrest (SCA), affect ~17.9 million people globally [1]-[3]. The AFib is most common type of heart arrhythmia, and the symptoms of AFib may be intermittent. Sudden cardiac arrest (SCA) often leads to sudden cardiac death (SCD). Nearly 70% of incidents occur at home. Thus, detection requires continuous and reliable healthcare monitoring.

Electrocardiography (ECG) has been a dominant cardiac monitoring technique for decades to identify cardiovascular abnormalities. Photoplethysmography (PPG) also contains valuable health-related information, such as blood oxygen, blood pressure, respiratory rate, etc., showing itself to be an alternative way to accommodate for the conditions where motion artifacts override ECG signals. Typically, PPG is obtained by illuminating the skin with the light from a light-emitting diode (LED) and then measuring the amount of light either transmitted or reflected to a photodiode (PD) [4]. The standard management of the cardiovascular conditions requires patients to visit healthcare facilities. Thus, the measurements of ECG/PPG are only collected during the sporadic visits. This is prone to missing the detection of the intermittent symptoms. Thus, a great number of researchers have been devoting their efforts to develop various wearable solutions (i.e., chest patch, smart watch, smart shirt, etc.) to enable daily life continuous healthcare [5]-[12].

This work is supported in part by NSF Award ECCS-2024486 and NSF ASSIST Center under Grant EEC-1160483.

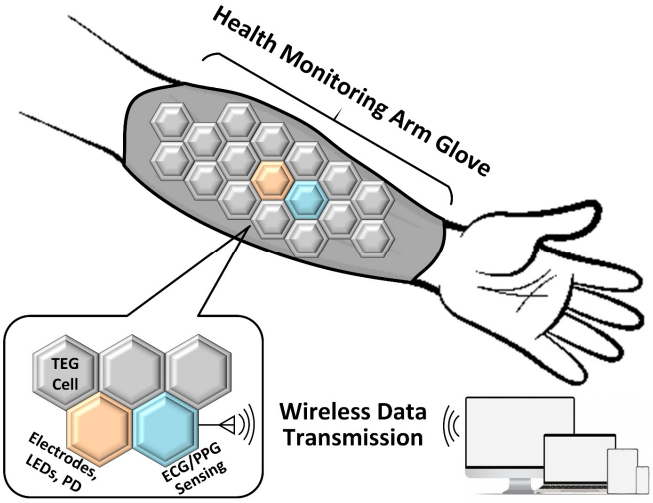

Fig. 1 Conceptual overview of a wearable solution for self-powered ECG and PPG sensing.

Recently, a few battery-powered wearable devices with multiple functionalities have been reported. In [5], a wristband benefiting from the proposed system-on-chip (SoC) design can perform multi-modal healthcare monitoring. In [6], the proposed SoC enables a compact health patch to be multifunctional. In [7], a wearable adaptive platform, which consists of spirometer, chest patch, and wristband, is able to track both environmental exposure and health condition. All these devices show their distinct advantage of having rich sensing capabilities, including ECG sensing, PPG sensing, skin-impedance monitoring, and body movement estimation. However, the limited lifetime of battery restricts the operation duration of the wearable device, especially when a power consuming application is involved. If a large battery is used to extent the device operation time, the wearability of device will be reduced.

Energy harvesting is a promising approach to realize self-powered wearable devices that run continuously without battery [8]-[12]. In [8], a body sensor node that harvests energy from TEG supports applications of electromyography (EMG), electroencephalography (EEG), and ECG sensing. In [9], the device powered by body heat using TEG can detect heart beats from ECG in the presence of motion artifacts. In the health monitoring system presented in [10], a sensor chip wirelessly powered through an inductive link performs ECG sensing. In [11], a Bionode device, which is capable of RF energy harvesting, monitoring EMG, enable upper limb

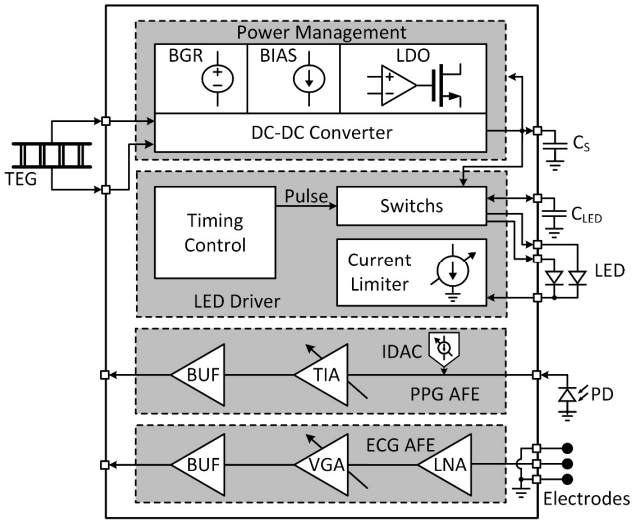

Fig. 2 Block diagram of the proposed SoC

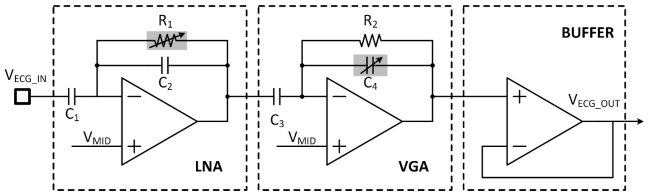

Fig. 3 Schematic diagram of the ECG AFE

prosthesis control. In [12], the authors proposed a SoC powered by TEG and/or photovoltaic cells (PV) to perform heart rate monitoring and body movement detection. These devices eliminate the need of charging and replacing battery allowing for long-term continuous health monitoring. However, the highly-constrained power budget prevents these devices from performing power-consuming application, particularly PPG sensing. Typically, to apply PPG measurement, LED illumination requires several mA to hundreds mA pulsed current for the intensity of light to be detectable by the PD. Thus, operating PPG sensing is a big challenge for a wearable device with limited power budget.

In this paper, we are demonstrating a novel SoC design, an important step towards a self-powered health sensing arm glove. The SoC performs both ECG and PPG sensing using the harvested power through TEG. The SoC utilizes the switch-capacitor-based architecture for power-efficient LED driving by periodically discharging the storage capacitor into the LED, which requires high instantaneous power to emit sufficient light. Fig. 1 shows the conceptual view of the self-powered arm glove, which incorporates TEG cells, electrodes, LEDs, photodiode (PD), microcontroller, and the proposed SoC. A large number of flexible TEG cells spreading over the glove collect energy generated by human heat and provide the SoC with the harvested power. The SoC steps up the TEG output voltage for being further regulated to power the sensing functions. This SoC includes functions of amplifying/filtering the recorded ECG signals from the electrodes, driving LED to emit enough light, and reading the resulting PD current to measure PPG. A microcontroller is needed to incorporate with the SoC for data digitization and wireless data transmission this time. The sensory data will be wirelessly sent to a data receiver (e.g., PC, smart phone, etc.) for data processing and

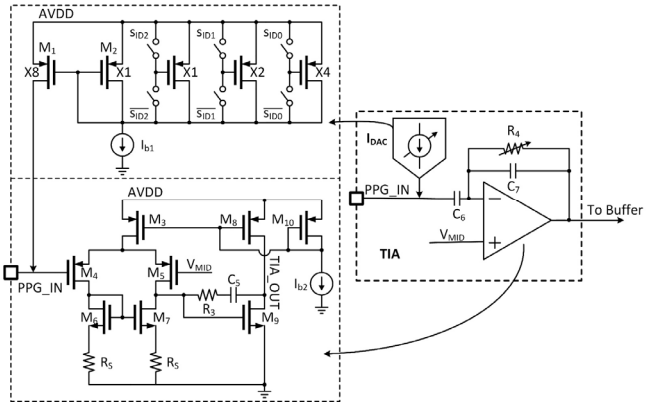

Fig. 4 Schematic diagram for the PPG AFE

real-time data display. The data digitization and transmission functions will be implemented in our next generation of SoC to eliminate the usage of the microcontroller.

II. SoC Architecture

The block diagram of the SoC is shown in Fig. 2. In the power management unit, an inductor-less DC-DC converter can start operating at an input voltage as low as 350 mV and produce a regulated and optimized output voltage of 2.1 V. Then, the low-dropout regulator (LDO), bandgap reference generator (BGR), and bias generator produce the supply voltage and bias current/voltage for the rest of the SoC. The ECG AFE includes three stages, a low-noise amplifier (LNA), a variable-gain-amplifier (VGA), and a buffer. In the LED driver, the timing control circuit controls charging the storage capacitor, C_{LED}, and discharging C_{LED} to the LED, while the current limiter sets the upper bound on the LED current. The PPG AFE, including a current-based digital-to-analog converter (IDAC), a transimpedance amplifier (TIA), and a buffer, converts and amplifies the PD current to a voltage signal.

A. ECG Analog-Front-End

The schematic diagram of the ECG AFE is shown in Fig. 3. The LNA based on the design in [13] is used as the first stage of the ECG AFE to decrease the noise figure. The DC blocking capacitor, C_1, removes the DC offset at the input. C_1 and C_2 set the gain of the LNA at 40 dB. R_1 and C_2 set the low-cut frequency of the ECG AFE. Given that implementing a large value of passive R_1 not only requires large chip area but also degrades noise performance, R_1 is a variable pseudo resistor referring to the design in [14]. Its resistance is able to be adjusted to change the low-cutoff frequency. To compensate the variation of input signal amplitude, the VGA is used as the second stage. C_4 is a 3-bit binary-weighted capacitor array. Its capacitance could be tuned to change the gain of VGA from 7 dB to 23 dB. A buffer is added to improve the ability of driving capacitive load, e.g., the capacitor arrays in a successive-approximation-register (SAR) analog-to-digital converter (ADC).

B. PPG Analog-Front-End

Fig. 4 shows the PPG AFE channel. The TIA converts and amplifies the PD current. The feedback resistor, R_4, is a 2-bit resistor array. The gain of the TIA is adjustable from 114 dBΩ to 120 dBΩ by changing the resistance of R_4. The core

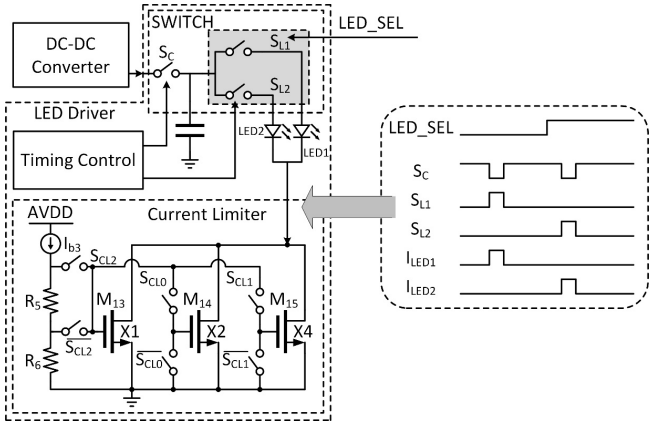

Fig. 5 Schematic diagram of the LED driver.

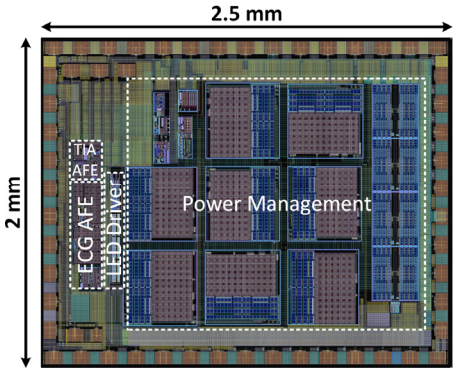

Fig. 6 Layout view of the proposed SoC.

amplifier of the TIA is a two-stage operational amplifier. The DC current offset at the input induced by the ambient light can saturate the TIA. To prevent the TIA from saturation, the 3-bit IDAC with adjustable output current from 1 µA to 8 µA can eliminate the ambient DC current at the input.

C. Switched-Capacitor-Based LED Driver

Driving a LED to emit sufficient light normally requires several mA to hundreds of mA pulsed current. The requirement of such high instantaneous power imposes a big challenge for the self-powered wearable device, which commonly has limited power budget. To achieve power-efficient LED driving under the tight power budget, we demonstrate a switched-capacitor-based LED driver [15] with details showed in Fig. 5.

In the charging phase, the DC-DC converter continuously charge the storage capacitor, C_{LED}, to the target voltage of 2.1 V by turning on the switch, S_C, while turning off both S_{L1} and S_{L2}. During this phase, C_{LED} accumulates energy to prepare for delivering current instantaneously to the LED. At the onset of the discharging phase, S_C is switched off to disconnect C_{LED} from the DC-DC converter while either S_{L1} or S_{L2} is switched on. The control bit, *LED_SEL*, determines which LED will be selected. C_{LED} damps charge to the selected LED, resulting in a large instantaneous current flowing through the LED without disturbing other blocks' normal operation. The key of the switch-capacitor-based operation is to prevent the main energy source from being loaded by the LED illuminating. The duration and frequency of the discharging phase are under control by the timing control block, resulting

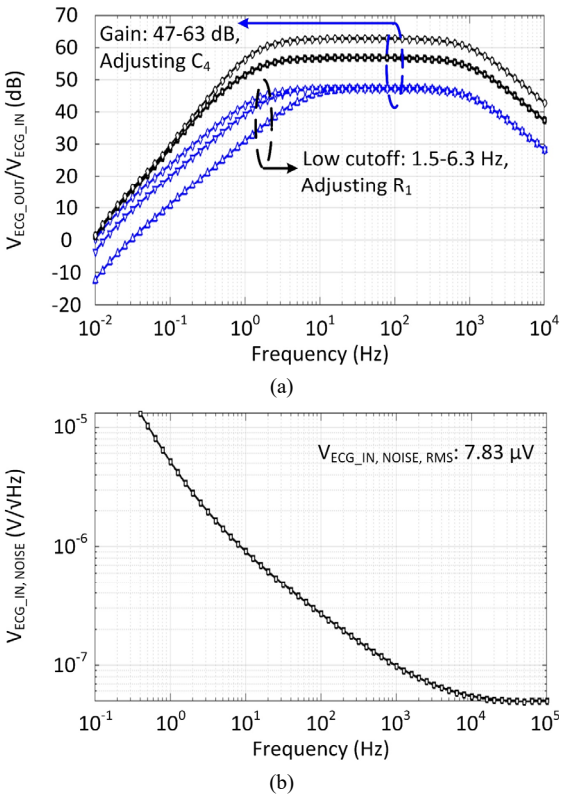

Fig. 7 (a) AC response and (b) input-referred noise spectrum of ECG AFE.

in the individually programmable pulse duration and frequency from 0.235 ms to 1.88 ms and from 7.8 Hz to 62.5 Hz, respectively. The LED current is limited by the current limiter, as shown in Fig. 5. The three control bits can set the upper bound of the LED current from 600 µA to 40 mA.

III. Post-Layout Simulation Results

The ECG/PPG sensor interface SoC was fabricated in the TSMC 0.18-µm 1P6M standard CMOS process, occupying a 2×2.5 mm^2 of silicon area including pads, as shown in Fig. 6. The functionality and performance of the SoC have been verified based on post-layout simulations. The ECG AFE has its low cut-off frequency in the range of 1.5 Hz–6.3 Hz, high cut-off frequency of 1.2 kHz, and gain in the range of 47 dB–63 dB, as shown in Fig. 7(a). The input-referred noise spectrum of the ECG AFE is shown in Fig. 7(b). Integration of this curve under the bandwidth of ECG AFE from 1.5 Hz to 1.2 kHz yields a root mean square (RMS) noise voltage of 7.83 μV_{RMS}. In Fig. 8, the PPG AFE shows its variable gain from 114 dBΩ to 120 dBΩ and a 119 pA_{RMS} input-referred RMS noise current.

In Fig. 9, the operation of the switch-capacitor-based LED driving is simulated with the discharging frequency of 32.5 Hz, duration of 1.5 ms, and LED current limit of 10 mA. C_{LED} is charged to 2.1 V, and dumps its charge to LED_1, creating an instantaneous current with its peak is limited to 10 mA. After the C_{LED} discharging phase, C_{LED} is recharged to be ready for the next discharging phase. Note that the LED driving operation has little effect on the output voltage of DC-DC converter, given that the C_{LED} is detached from the DC-DC converter during the discharging phase.

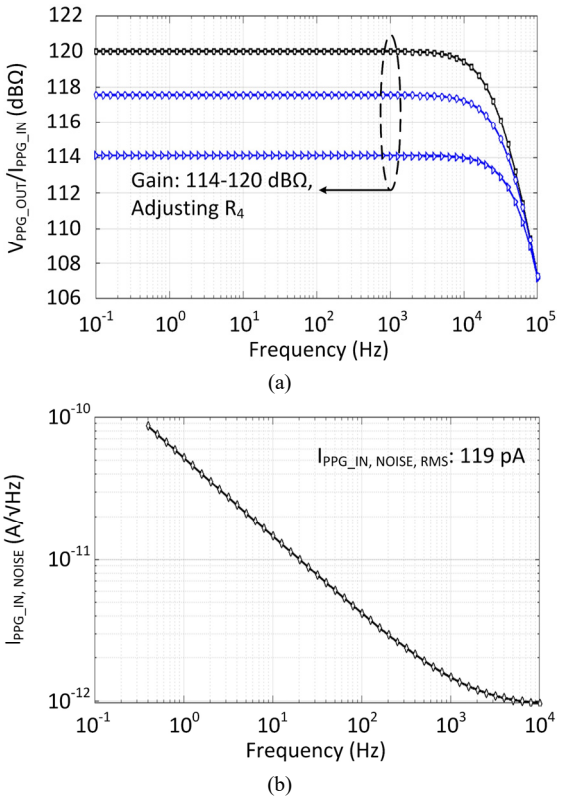

Fig. 8 (a) AC response and (b) input-referred noise spectrum of the PPG AFE.

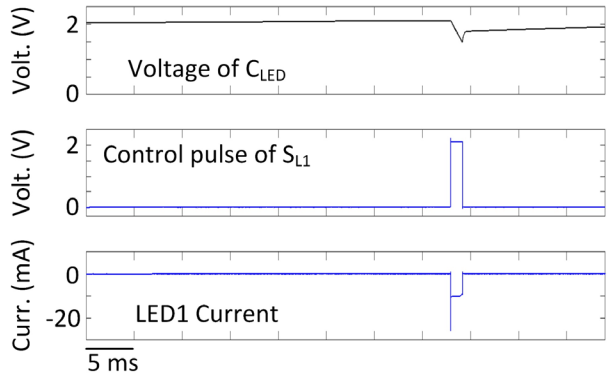

Fig. 9 Simulation results of the switch-capacitor-based LED driving operation.

IV. Conclusion

We have presented a dual-modal sensor interface SoC with specifications shown in Table I. The SoC is powered by the harvested energy from TEG, eliminating the need of battery. The DC-DC converter enables the SoC to start operating under low input voltage of 350 mV. Thanks to the switched-capacitor-based LED driver design, the SoC is able to provide high instantaneous current for the LED to emit with sufficient light, even though the power budget is limited. The SoC design is an important step towards a wearable device that can support not only ECG sensing but also the power-hungry PPG sensing while being powered by body heat. Such a wearable device will improve the development of the continuous and self-powered health monitoring technique.

TABLE I: POST-SIMULATED SOC SPECIFICATIONS

Overall system		
ASIC area		5 mm^2
System Voltages		2.1V (DC-DC output), 1.8V (System supply)
AFE	**ECG**	**PPG**
Low cutoff frequency	1.5-6.3 Hz, 2 bits	NA
Gain	47-63 dB, 2 bits	114-120 dBΩ, 2 bits
IDAC	NA	1-8 µA, 3 bits
Input-referred noise (RMS)	7.83 µV	119 pA
LED Driver		
Frequency		7.8-62.5 Hz, 2 bits
Pulse duration		0.235-1.88 ms, 3 bits
LED current		0.7-40 mA, 3 bits

References

[1] *AHA releases latest statistics on sudden cardiac arrest*, Sudden Cardiac Arrest Foundation, Feb. 2018. [Online]. Available: https://www.sca-aware.org/sca-news/aha-releases-latest-statistics-on-sudden-cardiac-arrest.

[2] *Atrial fibrillation*, Centers for Disease Control and Prevention, Sep. 2020. [Online]. Available: https://www.cdc.gov/heartdisease/atrial_fibrillation.htm

[3] *Cardiovascular diseases*, World Health Organization. [Online]. Available: https://www.who.int/health-topics/cardiovascular-diseases#tab=tab_1.

[4] K. Shelley, S. Shelley, and C. Lake, "Pulse oximeter waveform: photoelectric plethysmography," *Clinical monitoring,* pp. 420-428, 2001.

[5] M. Konijnenburg *et al.*, "A multi (bio) sensor acquisition System with integrated processor, power management, 8×8 LED drivers, and simultaneously synchronized ECG, BIO-Z, GSR, and two PPG readouts," *IEEE Journal of Solid-State Circuits,* vol. 51, no. 11, pp. 2584-2595, 2016.

[6] S. Song *et al.*, "A 769 µW battery-powered single-chip SoC with BLE for multi-modal vital sign monitoring health patches," *IEEE Transactions on Biomedical Circuits and Systems,* vol. 13, no. 6, pp. 1506-1517, 2019.

[7] J. Dieffenderfer *et al.*, "Low-power wearable systems for continuous monitoring of environment and health for chronic respiratory disease," *IEEE Journal of Biomedical and Health Informatics,* vol. 20, no. 5, pp. 1251-1264, 2016.

[8] Y. Zhang *et al.*, "A batteryless 19 µW MICS/ISM-band energy harvesting body sensor node SoC for ExG applications," *IEEE Journal of Solid-State Circuits,* vol. 48, no. 1, pp. 199-213, 2012.

[9] S. Bose, B. Shen, and M. L. Johnston, "A batteryless motion-adaptive heartbeat detection system-on-chip powered by human body heat," *IEEE Journal of Solid-State Circuits,* vol. 55, no. 11, pp. 2902-2913, 2020.

[10] J. Yoo, L. Yan, S. Lee, Y. Kim, and H.-J. Yoo, "A 5.2 mW self-configured wearable body sensor network controller and a 12 µW wirelessly powered sensor for a continuous health monitoring system," *IEEE Journal of Solid-State Circuits,* vol. 45, no. 1, pp. 178-188, 2009.

[11] H. Bhamra *et al.*, "A 24 µW, batteryless, crystal-free, multinode synchronized SoC "bionode" for wireless prosthesis control," *IEEE Journal of Solid-State Circuits,* vol. 50, no. 11, pp. 2714-2727, 2015.

[12] A. Roy *et al.*, "A 6.45 µW self-powered SoC with integrated energy-harvesting power management and ULP asymmetric radios for portable biomedical systems," *IEEE Transactions on Biomedical Circuits and Systems,* vol. 9, no. 6, pp. 862-874, 2015.

[13] R. R. Harrison and C. Charles, "A low-power low-noise CMOS amplifier for neural recording applications," *IEEE Journal of Solid-State Circuits,* vol. 38, no. 6, pp. 958-965, 2003.

[14] J. Dragas *et al.*, "In vitromulti-functional microelectrode array featuring 59760 electrodes, 2048 electrophysiology channels, stimulation, impedance measurement, and neurotransmitter detection channels," *IEEE Journal of Solid-State Circuits,* vol. 52, no. 6, pp. 1576-1590, 2017.

[15] Y. Jia, U. Guler, Y.-P. Lai *et al.*, "A trimodal wireless implantable neural interface system-on-chip," *IEEE Transactions on Biomedical Circuits and Systems*, vol. 14, no. 6, pp. 1207-1217, 2020